Preprint typeset in JHEP style - HYPER VERSION

CERN-TH-2003-150; IFUM-746/FT
FT-UM-TH-03-12; IFTM-03-10
ULB-TH/03-31

# The Neutrino mass matrix after Kamland and SNO salt enhanced results

**P. Aliani**[a], **V. Antonelli**[b,c], **M. Picariello**[b,c], **E. Torrente-Lujan**[d,e,f]

[a] *Service de Physique Théorique, Université Libre Bruxelles, Bruxelles, Belgium*
[b] *Dip. di Fisica, Università degli Studi di Milano, Milano, Italy*
[c] *I.N.F.N., Sezione di Milano, Milano, Italy*
[d] *Dept. de Fisica, Universidad de Murcia, Murcia, Spain*
[e] *Instituto de Fisica Teorica, Universidad de Murcia, Murcia, Spain*
[f] *CERN-TH Division, CH-1211 Geneve 23, Switzerland*
paola.aliani@ulb.ac.be, vito.antonelli@mi.infn.it,
marco.picariello@mi.infn.it, torrente@cern.ch

Abstract: An updated analysis of all available neutrino oscillation evidence in Solar experiments including the latest $SNOES, CC$ and $NC$ data (254d live time, NaCL enhanced efficiency) is presented. We obtain, for the fraction of active oscillating neutrinos: $\sin^2\alpha = (\Phi_{NC} - \Phi_{CC})/(\Phi_{SSM} - \Phi_{CC}) = 0.940^{+0.065}_{-0.060}$ nearly $20\sigma$ from the pure sterile oscillation case. The fraction of oscillating sterile neutrinos $\cos^2\alpha \lesssim 0.12$ ($1\sigma$ CL). At face value, these results might slightly favour the existence of a small sterile oscillating sector. In the framework of two active neutrino oscillations we determine individual neutrino mixing parameters and their errors and we obtain $\Delta m^2 = 7.01 \pm 0.08 \times 10^{-5}\mathrm{eV}^2, \quad \tan^2\theta = 0.42^{+0.12}_{-0.07}$. The main difference with previous analyses is a better resolution in parameter space. In particular the secondary region at larger mass differences (LMAII) is now excluded at 95% CL. The combined analysis of solar and Kamland data concludes that maximal mixing is not favoured at $\sim 4-5\sigma$. This is not supported by the antineutrino reactor results alone. We also estimate the individual elements of the two neutrino mass matrix, writing $M^2 = m^2 I + M_0^2$, we obtain ($1\sigma$ errors):

$$M_0^2 = 10^{-5}\ eV^2 \begin{pmatrix} 2.06^{+0.29}_{-0.31} & 3.15^{+0.29}_{-0.35} \\ 3.15^{+0.29}_{-0.35} & 4.60^{+0.56}_{-0.44} \end{pmatrix}.$$

Keywords: Neutrino Oscillations, Neutrino Mass matrix, SNO, Kamland.

## Contents

**1. Introduction** **1**

**2. Some Model Independent Results** **3**

**3. Methods and statistical procedures** **4**
3.1 Statistical Analysis 5

**4. Results and Discussion** **7**
4.1 An estimation of the neutrino mass matrix 8

**5. Summary and Conclusions** **9**

## 1. Introduction

The Sudbury Neutrino Observatory (SNO) collaboration has recently presented data relative to the NaCl phase of the experiment [1]. The addition of NaCl to a pure $D_2O$ detection medium increases the detector's sensitivity to the neutral-current (NC) reactions within its fiducial volume, enhancing the NC detection efficiency of about a factor three with respect to the previous 'no-salt' phase. This new result adds to a list of successive, compatible, ever more accurate results. The year 2002 was fundamental for neutrino physics and many long standing puzzles found their final solution. The data published in springtime by SuperKamiokande [2, 3] and SNO [4, 5] and the first results from the reactor experiment KamLAND [6] in December, confirmed the evidence accumulated in about 30 years of solar neutrino experiments, proved in a crystal clear way that neutrinos are massive and oscillating particles and selected the so-called Large Mixing Angle (LMA) between the different possible solutions of the Solar Neutrino Problem (SNP).

After the publication of the first KamLAND data a new era has started, in which the main issue is no longer to prove the validity of the oscillation hypothesis, but rather to determine with the best possible accuracy the oscillation parameters entering the PMNS mixing matrix. As it has been pointed out in previous papers (see for instance [7–10]), the accurate knowledge of the "solar mixing parameters" ($\theta_{12}$ and $\Delta m^2_{12}$ in the case of normal hierarchy) is essential not only for a better comprehension of this sector of neutrino physics, but also for the future study of the other mixing parameters.

In fact the neutrino parameters drive the subdominant effects in the long baseline and neutrino factory experiments and a lack of information about their exact values could seriously reduce the accuracy in the determination of the other elements of the mixing matrix and eventually of the CP violation parameter $\delta$. Hence, improving the present accuracy in the determination of the solar mixing parameters is mandatory not only to understand the physical potential of future experiments but also in order to optimize their set-up in the best possible way.

From this point of view, the situation was still quite unsatisfactory after the publication of the first KamLAND data. The many different analysis of these data [11–13] agree on the fact that these results, together with all the solar neutrino experiments, essentially select two distinct regions in the solar mixing parameter plan, both corresponding to the LMA solution. These two regions are usually denoted as "low LMA" and "high LMA". The mixing angle was not maximal, even if it was large and it was constrained in the interval $0.27 \leq \tan^2\theta_{12} \leq 0.88$ at the $3\sigma$ level. One can see that the uncertainty on the value of the mixing angle was still quite significant. Moreover it was not possible to discriminate between the two different possibilities for the mass difference. It is clear that a step further in the direction of pinning down more accurately the mixing parameters was needed.

The *SNO* experiment measures the $^8$B Solar neutrinos via the reactions [15–18]: 1) Charged Current (CC): $\nu_e + d \to 2p + e^-$, 2) Elastic Scattering (ES): $\nu_x + e^- \to \nu_x + e^-$. 3) Neutral Current(NC): $\nu_x + d \to p + n + \nu_x$. The first reaction is sensitive exclusively to electron neutrinos. The second, the same used in SuperKamiokande (SK), is instead sensitive, with different efficiencies, to all flavors. Finally the NC reaction is equally sensitive to all active neutrino species. Hence SNO can measure simultaneously the electron and active non-electron neutrino component of the solar flux at high energies ( $\gtrsim 5$ MeV). The novelty of the 'salt phase' is that it is now possible to distinguish clearly the NC events from the ES and CC ones and therefore to analyse the data without making use of the no-spectrum-distortion hypothesis [1, 19].

The non-electron component is found to be $\sim 5\sigma$ greater than zero, the standard prediction, thus providing the strongest evidence so far for flavour oscillation in the neutral lepton sector: the agreement of the total flux, provided by the NC measurement with the expectations implies as a by-product the confirmation of the validity of the SSM [20–22].

In this work we present an up-to-date analysis of all available Solar neutrino evidence, including the latest global SNO results [1] (together with the data of previous SNO phases [4, 5, 23] and of the other experiments [2, 24, 25], and of the KamLAND data [6]. A similar analysis using in addition the NaCl enhanced SNO spectrum will be presented elsewhere [14]. As a result, the new SNO data make the discrimination between the two different $\Delta m^2$ regions possible. In particular the secondary region at larger mass differences secondary region at larger mass differences (LMAII or high

LMA) is now excluded at 95% CL. The combined analysis of solar and KamLAND data continues to conclude that maximal mixing is not favored at an even larger significance level as before. Finally, we show that the achieved resolution in neutrino parameter space is good enough for an estimation of the individual elements of two neutrino mass matrix and their errors. As it will be shown below we obtain a square mass matrix:

$$M_0^2 = 10^{-5}\ eV^2 \begin{pmatrix} 2.06^{+0.29}_{-0.31} & 3.15^{+0.29}_{-0.35} \\ 3.15^{+0.29}_{-0.35} & 4.60^{+0.56}_{-0.44} \end{pmatrix}.$$

This result can be sharpened and a mass matrix can already be given if a concrete value for the absolute neutrino mass scale is assumed.

The structure of the present work is the following. First (section 2) we update some model independent results which put in a quantitative basis the extent of the deviations with respect to the standard non-oscillating case and the relative importance of active/sterile oscillations. After Section 3 dedicated to general description of methods, we determine (Section 4) the allowed areas in parameter space in the framework of active two neutrino oscillations from a standard statistical analysis. Individual values for $\Delta m^2$ and $\tan^2\theta$ with error estimation are obtained from the analysis of marginal likelihoods.

## 2. Some Model Independent Results

Different quantities can be defined in order to make the evidence for disappearance and appearance of the neutrino flavours explicit. From the three fluxes measured by SNO is possible to define two useful ratios, deviations of these ratios with respect to their standard value are powerful tests for occurrence of new physics. Here we update the computations of Ref.[26] for the values for $\Phi_{CC}/\Phi_{ES}$ and $\Phi_{CC}/\Phi_{NC}$ being extremely careful with the treatment of the correlations on the incertitudes. The inclusion or not of these correlations can affect significantly the results for these ratios (see table II in Ref.[1] for a complete list of systematical errors). The results we obtain from the new SNO data are similar to the old ones except for a strong decrease in the error bars in some cases. From the value from SNO rates[1] we obtain

$$\frac{\Phi_{CC}}{\Phi_{ES}} = 0.691^{+0.150}_{-0.096},$$

a value which is $\sim 2.1\ \sigma$ away from the no-oscillation expectation value of one. The ratio of CC and NC fluxes gives the fraction of electron neutrinos remaining in the solar neutrino beam at detection point. We obtain

$$\frac{\Phi_{CC}}{\Phi_{NC}} = 0.305^{+0.030}_{-0.024},$$

this value is nominally many standard deviations ($\sim 20\sigma$) away from the standard model case [27].

Finally, if in addition to SNO data we consider the flux predicted by the solar standard model one can obtain $\sin^2\alpha$, the fraction of active oscillating neutrinos, again using the SNO data and fully applying systematic correlations, we find:

$$\sin^2\alpha = \frac{\Phi_{NC}-\Phi_{CC}}{\Phi_{SSM}-\Phi_{CC}} = 0.940^{+0.065}_{-0.060} \quad (2.1)$$

$$\cos^2\alpha \lesssim 0.12 \quad (1\sigma), \quad (2.2)$$

where the fraction of oscillating sterile neutrinos $\cos^2\alpha \equiv 1-\sin^2\alpha$. The SSM flux is taken as the $^8$B flux predicted in the revised Ref.[21]. Although slightly increasing, the central value is still clearly below one (only-active oscillations case). Although electron neutrinos are still allowed to oscillate into sterile neutrinos the hypothesis of transitions to *only* sterile neutrinos is rejected at nearly $15\sigma$. On the other hand, as a consequence of the reduced error bars, this data can be taken as a mildly positive hint in favour of a small sterile component: the pure active case is now one sigma away from the central value (pure active oscillations are "excluded" at one sigma).

## 3. Methods and statistical procedures

The computation of the neutrino oscillation probabilities in Solar and Earth matter and of the expected signal in each experiment follows the standard methods found in the literature [28–36]. We solve numerically [29, 37], the neutrino evolution equations for all the oscillation parameter space. The survival probabilities for an electron neutrino, produced in the Sun, to arrive at the Earth are calculated in three steps. The propagation from the production point to sun's surface is computed numerically in all the parameter range using the electron number density $n_e$ given by the BPB2001 model [21] averaging over the production point. The propagation in vacuum from the Sun surface to the Earth is computed analytically. The averaging over the annual variation of the orbit is also exactly performed using simple Bessel functions. To take the Earth matter effects into account, we adopt a spherical model of the Earth density and chemical composition. In this model, the Earth is divided in eleven radial density zones [38], in each of which a polynomial interpolation is used to obtain the electron density. The composition of the neutrino propagation in the three different regions is performed exactly using an evolution operator formalism [36]. The final survival probabilities are obtained from the corresponding (non-pure) density matrices built from the evolution operators in each of these three regions. The night quantities are obtained using appropriate weights which depend on the neutrino impact parameter and the sagitta distance from neutrino trajectory to the Earth center, for each detector's geographical location. In this analysis in addition to night probabilities we will need the partial night probabilities corresponding to the 6 zenith angle bin data presented by SK [3]. They are obtained using appropriate weights which depend on

the neutrino impact parameter and the sagitta distance from neutrino trajectory to the Earth's center, for each detector's geographical location.

The expected signal in each detector is obtained by convoluting neutrino fluxes, oscillation probabilities, neutrino cross sections and detector energy response functions. We have used neutrino-electron elastic cross sections which include radiative corrections [39]. Neutrino cross sections on deuterium needed for the computation of the SNO measurements are taken from [40]. Detector effects are summarized by the respective response functions, obtained by taking into account both the energy resolution and the detector efficiency. We obtained the energy resolution function for SK using the data presented in [42–44]. The effective threshold efficiencies, which take into account the live time for each experimental period, are incorporated into our simulation program. They are obtained from [45]. The resolution function and other characteristics for SNO used here are those given in Refs.[1, 4, 5, 41].

The two principal ingredients in the calculation of the expected signal in KamLAND are the reactor flux and the antineutrino cross section on protons. We refer to Ref.[11] for a detailed account of the methods used here. In summary, in order to obtain the expected number of events at KamLAND, we sum the expectations for all the relevant reactor sources weighting each source by its power and distance to the detector (table II in Ref. [46] ), assuming the same spectrum originated from each reactor. We sum over the nearby power reactors, we neglect farther Japanese and Korean reactors and even farther rest-of-the-world reactors which give only a minor additional contribution. The average expected signal in each energy bin is given by the convolution of the oscillation probability averaged over the distance and power of the different reactors. Expressions for the antineutrino capture cross section are taken from the literature [47, 48]. The matrix element for this cross section can be written in terms of the neutron half-life, we have used the latest published value $t_{1/2} = 613.9 \pm 0.55$ [50]. The antineutrino flux spectrum, the relative reactor-reactor power normalization which is included in the definition of the effective probability and the energy resolution of KamLAND are used in addition. The energy resolution in the prompt positron detection is obtained by us from the raw calibration data presented in Ref.[11, 51]. Moreover, we assume a 408 ton fiducial mass and standard nuclear plant power and fuel schedule, we take an averaged, time-independent, fuel composition equal for each detector. Detection efficiency is taken close 100% and independent of the energy [6].

### 3.1 Statistical Analysis

The statistical significance of the neutrino oscillation hypothesis is tested with a standard $\chi^2$ method which is explained in detail in Ref.[29]. Our present analysis is based on the consideration of a $\chi^2$ sum of two distinct contributions, one coming from SNO global rates and all the rest of solar neutrino data and the contribution of the KamLAND experiment $\chi^2 = \chi^2_{\odot} + \chi^2_{KL}$. The contribution from KamLAND

includes the binned signal (See table 2 in Ref.[11]) as is explained in detail in Ref.[6]. In summary, the KamLAND contribution is made of two parts, one with $\chi^2_{gl,KL} = (R^{exp} - R^{th})^2/\sigma^2$. The experimental signal $R^{exp}$ and statistical and systematic errors are shown in Table 1. The contribution of the KamLAND spectrum is as follows:

$$\chi^2_{\rm spec,KL} = (\alpha \boldsymbol{R}^{\rm th} - \boldsymbol{R}^{\rm exp})^t \left(\sigma^2_{unc} + \sigma^2_{corr}\right)^{-1} (\alpha \boldsymbol{R}^{\rm th} - \boldsymbol{R}^{\rm exp}) \tag{3.1}$$

The total error matrix $\sigma$ is computed as a sum of assumed systematic deviations, $\sigma_{sys}/S \sim 6.5\%$, mainly coming from flux uncertainty (3%), energy calibration and threshold (see table II of Ref. [6]. for a total systematic error $\sim 6.4\%$), see also Ref.[46, 51, 56]) and statistical errors. The parameter $\alpha$ is a free normalization parameter. The effect of systematic sources on individual bin deviations has been computed by us studying the influence on the response function, furtherly we have assumed full correlation among bins.

The solar neutrino contribution can be written in the following way:

$$\chi^2_\odot = \chi^2_{\rm glob} + \chi^2_{\rm SK} + \chi^2_{\rm SNO}. \tag{3.2}$$

The function $\chi^2_{\rm glob}$ correspond to the total event rates measured at the Homestake experiment [24] and at the gallium experiments SAGE [52], GNO [53] and GALLEX [54]. We follow closely the definition used in previous works (see Ref.[26] for definitions and Table (1) in Ref.[26] for an explicit list of results and other references). The contribution to the $\chi^2$ from the SuperKamiokande data ($\chi^2_{\rm SK}$) has been obtained by using double-binned data in energy and zenith angle (see table 2 in Ref.[3] and also Ref.[2]): 8 energy bins of variable width and 7 zenith angle bins which include the day bin and 6 night ones (see Ref.[6]).

The contribution of SNO to the $\chi^2$ is given by $\chi^2_{SNO} = \chi^2_{gl,SNO} + \chi^2_{spec,SNO}$ where $\chi^2_{spec,SNO}$ is the spectrum contribution made up by the day and night values of the total (NC+CC+ES) SNO signal for the different values of the spectrum [11]. The new component corresponding to the individual global signals is given by

$$\chi^2_{\rm gl,SNO} = \sum_{i=ES,CC,NC} (\alpha \boldsymbol{R}^{\rm th} - \boldsymbol{R}^{\rm exp})^t \left(\sigma^2_{\rm stat} + \sigma^2_{\rm syst}\right)^{-1} (\alpha \boldsymbol{R}^{\rm th} - \boldsymbol{R}^{\rm exp}), \tag{3.3}$$

where the signal $\boldsymbol{R}$ vectors of dimension 3 are made up by the values of the total ES, CC, NC SNO signals. The statistical contribution to the covariance matrix, $\sigma_{\rm stat}$ is non-diagonal since the different fluxes are derived from a fit to a single data sample [1, 41]. The part of the matrix related to the systematical errors includes contributions from neutron capture efficiency and other geometrical inefficiencies appearing in the statistical separation of ES, CC and NC events as presented in Ref.[41].

## 4. Results and Discussion

To test a particular oscillation hypothesis against the parameters of the best fit and obtain allowed regions in parameter space we perform a minimisation of the three dimensional function $\chi^2(\Delta m^2, \tan^2\theta, \alpha)$. For $\alpha = \alpha_{\min}$, a given point in the oscillation parameter space is allowed if the globally subtracted quantity fulfills the condition $\Delta\chi^2 = \chi^2(\Delta m^2, \theta) - \chi^2_{\min} < \chi^2_n(CL)$. Where $\chi^2_{n=3}(90\%, 95\%, ...)$ are the quantiles for three degrees of freedom.

The results are shown in Figs.1 where we have generated acceptance contours in the $\Delta m^2$-$\tan^2\theta$ plane. In Fig.2 we present the same results as in Fig.1 but using linear scales. The resolution in the neutrino parameter space has become good enough for this to become useful. With the actual experimental precision we can assert that the mixing parameters are now known much better than as order of magnitude only. In Table (2) we present the best fit parameters or local minimum obtained from the minimisation of the full $\chi^2$ function.

The main difference with previous analysis is a better resolution in parameter space. The previously two well separated solutions LMAI,LMAII have now disappeared. In particular the secondary region at larger mass differences (LMAII) is now excluded at 95% CL.

The introduction of the new solar data in general strongly diminishes the favored value for the mixing angle with respect to the KamLAND result alone [11]. The final value is more near to those values favored by the solar data alone than to the KamLAND ones. As an important consequence, the combined analysis of solar and KamLAND data concludes that maximal mixing is not favored at $\sim 4 - 5\sigma$. This conclusion is not supported by the antineutrino, earth-controlled, conceptually simpler KamLAND results alone. As we already pointed out in Ref.[11], this effect could be simply due to the present low KamLAND statistics or, more worrying, to some statistical artifact derived from the complexity of the analysis and of the heterogeneity of binned data involved.

Additionally, we perform a second kind of analysis in order to obtain concrete values for the individual oscillation parameters and estimates for their uncertainties. We study the marginalised parameter constraints where the $\chi^2$ quantity is converted into likelihood using the expression $\mathcal{L}/\mathcal{L}_0 = e^{-(\chi^2-\chi^2_{min})/2}$. This normalized marginal likelihood, obtained from the integration of $\mathcal{L}$ for each of the variables, is plotted in Figs. (3) for each of the oscillation parameters $\Delta m^2$ and $\tan^2\theta$. Concrete values for the parameters are extracted by fitting one- or two-sided Gaussian distributions to any of the peaks (fits not showed in the plots). In both cases, for angle and the mass difference distributions the goodness of fit of the Gaussian fit to each individual peak is excellent (g.o.f $\sim 100\%$). The values for the parameters obtained in this way appear in Table 2. The errors obtained from this method are assigned to the $\chi^2$ minimisation values. The central values are fully consistent and very similar to the

values obtained from simple $\chi^2$ minimisation. In particular, the maximal mixing solution is again excluded at the $\sim 4-5\sigma$ level. A common feature to previous analysis presented by us [11] is that, although both are mutually compatible, the slight difference of the value obtained for the mixing angle is well explained by the shape of the allowed regions in Fig 1 (right): the right elongation of these shift the value of the integral which defines the marginal distribution for $\tan^2\theta$. Additional variability can be easily introduced if would have used different prior information or mixing parameterizations.

We will again use the technique of marginal distributions in the next paragraphs to obtain an estimation of the individual elements of the neutrino mass matrix and their errors.

### 4.1 An estimation of the neutrino mass matrix

The square of the neutrino mass matrix can be written in the flavour basis as $M^2 = UM_D^2U^\dagger$ where $M_D$ is diagonal and $U$ is an unitary (purely active oscillations are assumed) mixing matrix. Subtracting one of the diagonal entries we have

$$M^2 = m_1^2 I + M_0^2 = m_1^2 I + UM_D'^2U^\dagger,$$

where $I$ is the identity matrix. In this way we distinguish in the mass matrix a part, $M_0^2$, which affects and can be determined by oscillation experiments and another one, $m_1^2 I$, which does not. Evidently, the off-diagonal elements of the mass matrix are fully measurable by oscillation experiments.

Restricting ourselves for the sake of simplicity to two neutrino oscillations, we have

$$M^2 = m_1^2 I + M_0^2 = m_1^2 I + \Delta m^2 \begin{pmatrix} \sin^2\theta & \sin\theta\cos\theta \\ \sin\theta\cos\theta & \cos^2\theta \end{pmatrix} \tag{4.1}$$

with $\Delta m^2 = m_2^2 - m_1^2$. The individual elements of the matrix $M_0$ can simply be estimated from the oscillation parameters obtained before. For example for $\tan^2\theta \sim 0.40$, $\Delta m^2 \sim 7\times 10^{-5}\ eV^2$ we would obtain $(M_0^2)_{22} \sim 5\times 10^{-5}\ eV^2$.

Our objective is however to estimate how well the individual errors of the mass matrix can be extracted already at present by the existing experimental evidence. For this purpose we have applied similar arguments as those used before to obtain marginal distributions and errors for individual parameters from them. Using again as likelihood function the quantity $\mathcal{L}/\mathcal{L}_0(\Delta m^2, \tan^2\theta) = e^{-(\chi^2-\chi^2_{min})/2}$ we obtained the individual probability distributions for any of the elements of the matrix $M_0$. Average values and $1\sigma$ errors are obtained from two-sided Gaussian fits to these distributions.

From this procedure we obtain:

$$M_0^2 = 10^{-5}\ eV^2 \begin{pmatrix} 2.06^{+0.29}_{-0.31} & 3.15^{+0.29}_{-0.35} \\ 3.15^{+0.29}_{-0.35} & 4.60^{+0.56}_{-0.44} \end{pmatrix}. \tag{4.2}$$

One can go further supposing a concrete value for $m_1^2$ from elsewhere. If we take $m_1^2 >> \Delta m^2$ then we can directly write the mass matrix

$$M = m_1 I + \frac{1}{2m_1} M_0^2. \tag{4.3}$$

Supposing for example $m_1 = 1\ eV$,

$$M = eV \begin{pmatrix} 1.00 + 1.03^{+0.15}_{-0.15}\ 10^{-5} & 1.60^{+0.15}_{-0.17}\ 10^{-5} \\ 1.60^{+0.15}_{-0.17}\ 10^{-5} & 1.00 + 4.60^{+0.56}_{-0.44}\ 10^{-5} \end{pmatrix}. \tag{4.4}$$

this is the final two neutrino mass matrix which can be obtained from present oscillation evidence coming from solar and reactor neutrinos.

## 5. Summary and Conclusions

In this work we have presented an up-to-date analysis of all available Solar neutrino evidence including latest SNO results with NaCl enhanced efficiency in the most simple framework. The increasingly accurate direct measurement via the $NC$ reaction on deuterium of $^8$B neutrinos combined with the $CC$ results have largely confirmed the neutrino oscillation hypothesis.

In a model independent basis, We obtain the following values for the ratios: $\Phi_{CC}/\Phi_{NC} = 0.305^{+0.030}_{-0.024}$, $\Phi_{CC}/\Phi_{ES} = 0.691^{+0.150}_{-0.096}$. The fraction a of oscillating neutrinos into active and sterile ones are computed to be:

$$\sin^2\alpha = 0.940^{+0.065}_{-0.060}, \quad \cos^2\alpha \lesssim 0.12\ (1\sigma), \tag{5.1}$$

where the fraction of oscillating sterile neutrinos $\cos^2\alpha \equiv 1 - \sin^2\alpha$. Although slightly increasing, the central value is still clearly below one, the only-active oscillations case. The hypothesis of transitions to *only* sterile neutrinos is well rejected but, as a consequence of the reduced error bars, this data can be taken as a mildly positive hint in favour of a small sterile component: the pure active case is now one sigma away from the central value.

We have obtained the allowed area in parameter space and individual values for $\Delta m^2$ and $\tan^2\theta$ with error estimation from the analysis of marginal likelihoods. We have shown that it is already possible to determine at present active two neutrino oscillation parameters with relatively good accuracy. In the framework of two active neutrino oscillations we obtain

$$\Delta m^2 = 7.01 \pm 0.08 \times 10^{-5}\mathrm{eV}^2, \quad \tan^2\theta = 0.42^{+0.12}_{-0.07}.$$

The combined analysis of solar and KamLAND data concludes that maximal mixing is not favored at $\sim 4 - 5\sigma$. This conclusion is not supported by the antineutrino, earth-controlled, conceptually simpler KamLAND results alone.

We estimate the individual elements of the two neutrino mass matrix, we show that individual elements of this matrix can be determined with an error $\sim 10\%$ from present experimental evidence.

**Acknowledgments**

It is a pleasure to thank R. Ferrari for many enlightening discussions and for his encouraging and material support. We acknowledge the financial support of the Italian MIUR, the Spanish CYCIT funding agencies and the CERN Theoretical Division. P.A. acknowledges funding from the Inter-University Attraction Pole (IUAP) "fundamental interactions". The numerical calculations have been performed in the computer farm of the Milano University theoretical group.

## References

[1] S. N. Ahmed *et al.*, ArXiv:nucl-ex/0309004, [see `http://www.sno.phy.queensu.ca`]

[2] S. Fukuda *et al.* [Super-Kamiokande Collaboration], Phys. Lett. B **539** (2002) 179.

[3] M. B. Smy, arXiv:hep-ex/0202020.

[4] Q. R. Ahmad *et al.* [SNO Collaboration], Phys. Rev. Lett. **89**, 011302 (2002).

[5] Q. R. Ahmad *et al.* [SNO Collaboration], Phys. Rev. Lett. **89**, 011301 (2002).

[6] K. Eguchi *et al.* [KamLAND Collaboration], *"First results from KamLAND: Evidence for reactor anti-neutrino disappearance,"* Phys. Rev. Lett. **90**, 021802 (2003).

[7] P. Migliozzi and F. Terranova, Phys. Lett. B **563** (2003) 73.

[8] A. Bandyopadhyay, S. Choubey and S. Goswami, Phys. Rev. D **67** (2003) 113011.

[9] J. N. Bahcall and C. Pena-Garay, arXiv:hep-ph/0305159.

[10] S. Choubey, S. T. Petcov and M. Piai, arXiv:hep-ph/0306017.

[11] P. Aliani, V. Antonelli, M. Picariello and E. Torrente-Lujan, Phys. Rev. D Vol. 68 (2003) 053000 [arXiv:hep-ph/0212212].

[12] G. L. Fogli, E. Lisi, A. Marrone, D. Montanino, A. Palazzo and A. M. Rotunno, Phys. Rev. D **67** (2003) 073002; V. Barger and D. Marfatia, Phys. Lett. B **555** (2003) 144; M. Maltoni, T. Schwetz and J. W. Valle, Phys. Rev. D **67** (2003) 093003; J. N. Bahcall, M. C. Gonzalez-Garcia and C. Pena-Garay, JHEP **0302** (2003) 009; A. Bandyopadhyay, S. Choubey, R. Gandhi, S. Goswami and D. P. Roy, Phys. Lett. B **559** (2003) 121; W. l. Guo and Z. z. Xing, Phys. Rev. D **67** (2003) 053002; P. C. de Holanda and A. Y. Smirnov, JCAP **0302** (2003) 001; G. L. Fogli, E. Lisi,

A. Marrone, D. Montanino, A. Palazzo and A. M. Rotunno, arXiv:hep-ph/0308055; T. Schwetz, arXiv:hep-ph/0308003; H. Nunokawa, W. J. Teves and R. Zukanovich Funchal, Phys. Lett. B **562** (2003) 28; G. Barenboim, L. Borissov and J. Lykken, arXiv:hep-ph/0212116; A. Y. Smirnov, arXiv:hep-ph/0306075; M. C. Gonzalez-Garcia and C. Pena-Garay, arXiv:hep-ph/0306001; A. Ianni, J. Phys. G **29** (2003) 2107; A. B. Balantekin and H. Yuksel, J. Phys. G **29** (2003) 665; S. Pakvasa and J. W. Valle, arXiv:hep-ph/0301061.

[13] V. Antonelli, F. Caravaglios, R. Ferrari and M. Picariello, Phys. Lett. B **549** (2002) 325 [arXiv:hep-ph/0207347]. V. Antonelli, F. Caravaglios, R. Ferrari and M. Picariello, arXiv:hep-ph/0305169.

[14] P. Aliani, V. Antonelli, M. Picariello and E. Torrente-Lujan, In preparation.

[15] J. R. Klein [SNO Collaboration], *In *Venice 1999, Neutrino telescopes, vol. 1* 115-125.* A. B. McDonald [SNO Collaboration], Nucl. Phys. Proc. Suppl. **77** (1999) 43.

[16] J. Boger *et al.* [SNO Collaboration], Nucl. Instrum. Meth. A **449** (2000) 172.

[17] V. Barger, D. Marfatia and K. Whisnant, Phys. Lett. B **509** (2001) 19.

[18] J. N. Bahcall, P. I. Krastev and A. Y. Smirnov, JHEP **0105** (2001) 015.

[19] G. L. Fogli, E. Lisi, A. Marrone and A. Palazzo, arXiv:hep-ph/0309100; A. B. Balantekin and H. Yuksel, arXiv:hep-ph/0309079; M. Maltoni, T. Schwetz, M. A. Tortola and J. W. Valle, arXiv:hep-ph/0309130. H. Murayama and C. Pena-Garay, arXiv:hep-ph/0309114.

[20] S. Turck-Chieze, Nucl. Phys. Proc. Suppl. **91** (2001) 73. E. G. Adelberger *et al.*, Rev. Mod. Phys. **70** (1998) 1265. A. S. Brun, S. Turck-Chieze and P. Morel, arXiv:astro-ph/9806272.

[21] J. N. Bahcall, M. H. Pinsonneault and S. Basu, Astrophys. J. **555**, 990 (2001).

[22] J.N. Bahcall and M.H. Pinsonneault, Rev. Mod. Phys. **67** (1995) 781.

[23] Q. R. Ahmad *et al.* [SNO Collaboration], Phys. Rev. Lett. **87** (2001) 071301.

[24] R. Davis, Prog. Part. Nucl. Phys. 32 (1994) 13; B.T. Cleveland et al., (HOMESTAKE Coll.) Nucl. Phys. (Proc. Suppl.)**B 38** (1995) 47; B.T. Cleveland et al., (HOMESTAKE Coll.) Astrophys. J. 496 (1998) 505-526.

[25] V. Gavrin, 4th International Workshop on Low Energy and Solar Neutrinos, Paris, May19-21,2003 ; T. Kirsten, *Progress in GNO*, XXth Int. Conf. on Neutrino Physics and Astrophysics, Munich, May 25-30, 2002; to be published in Nucl. Phys. (Proc. Suppl.)**B**

[26] P. Aliani, V. Antonelli, R. Ferrari, M. Picariello and E. Torrente-Lujan, Phys. Rev. D **67** (2003) 013006 [arXiv:hep-ph/0205053].

[27] Y. Fukuda *et al.* [Super-Kamiokande Collaboration], Phys. Rev. Lett. **82**, 1810; J. N. Bahcall, P. I. Krastev and E. Lisi, Phys. Rev. C **55**, 494 (1997); J. N. Bahcall and E. Lisi, Phys. Rev. D **54**, 5417 (1996).

[28] V. Barger, D. Marfatia and K. Whisnant, arXiv:hep-ph/0106207

[29] P. Aliani, V. Antonelli, M. Picariello and E. Torrente-Lujan, Nucl. Phys. B **634** (2002) 393; P. Aliani, V. Antonelli, M. Picariello and E. Torrente-Lujan, Nucl. Phys. Proc. Suppl. **110**, 361 (2002); E. Torrente Lujan, Phys. Rev. D **53**, 4030 (1996). P. Aliani, V. Antonelli, R. Ferrari, M. Picariello and E. Torrente-Lujan, arXiv:hep-ph/0206308. P. Aliani, V. Antonelli, R. Ferrari, M. Picariello and E. Torrente-Lujan, arXiv:hep-ph/0205061.

J. N. Bahcall, E. Lisi, D. E. Alburger, L. De Braeckeleer, S. J. Freedman and J. Napolitano, Phys. Rev. C **54**, 411 (1996).

[30] G. L. Fogli, E. Lisi, D. Montanino and A. Palazzo, Phys. Rev. D **64** (2001) 093007.

[31] P. I. Krastev and A. Y. Smirnov, arXiv:hep-ph/0108177.

[32] J. N. Bahcall, M. C. Gonzalez-Garcia and C. Pena-Garay, JHEP **0108**, 014 (2001); J. N. Bahcall, M. C. Gonzalez-Garcia and C. Pena-Garay, [arXiv:hep-ph/0111150]

[33] A. Bandyopadhyay, S. Choubey, S. Goswami and K. Kar, arXiv:hep-ph/0110307.

[34] S. Choubey, S. Goswami and D. P. Roy, arXiv:hep-ph/0109017.

[35] A. Bandyopadhyay, S. Choubey, S. Goswami and K. Kar, Phys. Lett. B **519** (2001) 83.

[36] E. Torrente-Lujan, Phys. Rev. D **59** (1999) 093006. E. Torrente-Lujan, Phys. Rev. D **59** (1999) 073001. E. Torrente-Lujan, Phys. Lett. B **441** (1998) 305. V. B. Semikoz and E. Torrente-Lujan, Nucl. Phys. B **556** (1999) 353. E. Torrente-Lujan, Phys. Lett. B **494** (2000) 255. E. Torrente-Lujan, arXiv:hep-ph/9902339. S. Khalil and E. Torrente-Lujan, J. Egyptian Math. Soc. **9**, 91 (2001) [arXiv:hep-ph/0012203].

[37] P. Aliani, V. Antonelli, M. Picariello and E. Torrente-Lujan, arXiv:cs.ce/0307053.

[38] I. Mocioiu and R. Shrock, Phys. Rev. D **62** (2000) 053017; A. Dziewonski, in *The Encyclopedia of Solid Earth Geophysics*, edited by D.E James (Van Nostrand Reinhold, New York 1989).

[39] J. Bahcall, M. Kamionkowski, A. Sirlin, Phys. Rev. D51 (1995) 6146; M. Passera, Phys. Rev. D. 64 (2001) 113002 .

[40] S. Nakamura, T. Sato, V. Gudkov and K. Kubodera, Phys. Rev. C **63** (2001) 034617.

[41] Q. R. Ahmad *et al.* [SNO Collaboration], "HOWTO use the SNO solar Neutrino Spectral data", http://www.sno.phy.queensu.ca/sno.

[42] M. Nakahata *et al.* [SK Coll.], Nucl. Instrum. Meth. A **421**, 113 (1999).

[43] H. Ishino, Ph. D. thesis, University of Tokio,1999. M. Nakahata et al. (SK Coll.), Nucl. Instrum. Methods 46 (1998) 301.

[44] N. Sakurai, Ph.D. Thesis, Dec. 2000 *Constraints of the neutrino oscillation parameters from 1117 day observation of soloar neutrino day and night spectra in Super-Kamiokande.*

[45] S. Fukuda *et al.* [SK Coll.], Phys. Rev. Lett. **86**, 5651 (2001).

[46] H. Murayama and A. Pierce, Phys. Rev. D **65** (2002) 013012.

[47] P. Vogel and J. F. Beacom, Phys. Rev. D **60**, 053003 (1999).

[48] P. Aliani, V. Antonelli, M. Picariello and E. Torrente-Lujan, JHEP **0302** (2003) 025. E. Torrente-Lujan, JHEP **0304** (2003) 054 [arXiv:hep-ph/0302082]. B. C. Chauhan, J. Pulido and E. Torrente-Lujan, Phys. Rev. D **68** (2003) 033015 [arXiv:hep-ph/0304297].

[49] P. Aliani, V. Antonelli, M. Picariello and E. Torrente-Lujan, New J. Phys. **5** (2003) 2 [arXiv:hep-ph/0207348]. P. Aliani, V. Antonelli, R. Ferrari, M. Picariello and E. Torrente-Lujan, reactor neutrino physics," AIP Conf. Proc. **655** (2003) 103 [arXiv:hep-ph/0211062].

[50] "Review of Particle Properties", K. Hagiwara et al. (Particle Data Group), Phys. Rev. D 66 (2002) 010001

[51] G.Horton-Smith, *Neutrinos and Implications for Physics Beyond the Standard Model,* Stony Brook, Oct. 11-13, 2002. http://insti.physics.sunysb.edu/itp/conf/neutrino.html

[52] A.I. Abazov et al. (SAGE Coll.), Phys. Rev. Lett. **67** (1991) 3332. D.N. Abdurashitov et al. (SAGE Coll.), Phys. Rev. Lett. **77** (1996) 4708. J.N. Abdurashitov et al., (SAGE Coll.), Phys. Rev. **C60** (1999) 055801; astro-ph/9907131. J.N. Abdurashitov et al., (SAGE Coll.), Phys. Rev. Lett. **83** (1999) 4686.

[53] M. Altmann et al. (GNO Coll.) Phys. Lett. B490 (2000) 16-26.

[54] P. Anselmann et al., GALLEX Coll., Phys. Lett. **B 285** (1992) 376. W. Hampel et al., GALLEX Coll., Phys. Lett. **B 388** (1996) 384. T.A. Kirsten, Prog. Part. Nucl. Phys. 40 (1998) 85-99. W. Hampel et al., (GALLEX Coll.) Phys. Lett. **B 447** (1999) 127. M. Cribier, Nucl. Phys. (Proc. Suppl.)**B 70** (1999) 284. W. Hampel et al., (GALLEX Coll.) Phys. Lett. **B 436** (1998) 158. W. Hampel et al., (GALLEX Coll.) Phys. Lett. **B 447** (1999) 127.

[55] K. Lande (For the Homestake Coll.) Nucl. Phys. B(Proc. Suppl.)77(1999)13-19.

[56] J. Shirai, "Start of Kamland", talk given at *Neutrino 2002*, XXth International Conference on Neutrino Physics and Astrophysics, May 2002, Munich, `http://neutrino2002.ph.tum.de`. See also: P. Alivisatos *et al.*, STANFORD-HEP-98-03.

| Experiment [Ref.] | $S_{Data}$ | $S_{Data}/S_{SSM}$ ($\pm 1\sigma$) |
|---|---|---|
| New SNO data[1]: | | |
| SNO-ES | $2.21 \pm 0.28 \pm 0.10$ | $0.406 \pm 0.091$ |
| SNO-CC | $1.59 \pm 0.08 \pm 0.07$ | $0.292 \pm 0.056$ |
| SNO-NC | $5.21 \pm 0.27 \pm 0.38$ | $0.958 \pm 0.193$ |
| Other Solar data: | | |
| $D_2O$ SNO-ES [4, 5] | $2.39 \pm 0.23 \pm 0.12$ | $0.439 \pm 0.092$ |
| $D_2O$ SNO-CC [4, 5] | $1.76 \pm 0.05 \pm 0.09$ | $0.324 \pm 0.054$ |
| $D_2O$ SNO-NC [4, 5] | $5.09 \pm 0.43 \pm 0.45$ | $0.936 \pm 0.208$ |
| SK [2] | $2.32 \pm 0.03 \pm 0.08$ | $0.451 \pm 0.011$ |
| Cl [55] | $2.56 \pm 0.16 \pm 0.16$ | $0.332 \pm 0.056$ |
| SAGE [52] | $67.2 \pm 7.0 \pm 3.2$ | $0.521 \pm 0.067$ |
| GNO-GALLEX [53, 54] | $74.1 \pm 6.7 \pm 3.5$ | $0.600 \pm 0.067$ |

**Table 1:** Summary of data used in this work. The observed signal ($S_{Data}$) and ratios $S_{Data}/S_{SSM}$ with respect to the BPB2001 model are reported. The SK and SNO rates are in $10^6$ cm$^{-2}$ s$^{-1}$ units. The Cl , SAGE and GNO-GALLEX measurements are in SNU units. In this work we use the combined results of SAGE and GNO-GALLEX: $S_{\rm Ga}/S_{\rm SSM}$ (Ga $\equiv$ SAGE+GALLEX+GNO)=$0.579 \pm 0.050$. The SSM $^8$B total flux is taken from the (revised) BPB2001 model [21]: $\Phi_\nu(^8\text{B}) = 5.44(1^{+0.20}_{-0.16}) \times 10^6$ cm$^{-2}$ s$^{-1}$. In addition we have used from reactor Kamland measurements the signal ratio $R = 0.611 \pm 0.085 \pm 0.041$ [6]and its signal spectrum [6, 11].

| | $\Delta m^2(\text{eV}^2)$ | $\tan^2\theta$ |
|---|---|---|
| From minimization $\chi^2$: | $7.01 \times 10^{-5}$ | 0.42 |
| From Marg. Fit, ( $\pm 1\sigma$): | $7.30^{+0.08}_{-0.08} \times 10^{-5}$ | $0.46^{+0.12}_{0.07}$ |

**Table 2:** Mixing parameters: from $\chi^2$ minimization, $\chi^2/ndf = 0.94$ (Fig. 1 right) and from double-sided fit to the peak of marginal likelihood distributions (Figs.3).

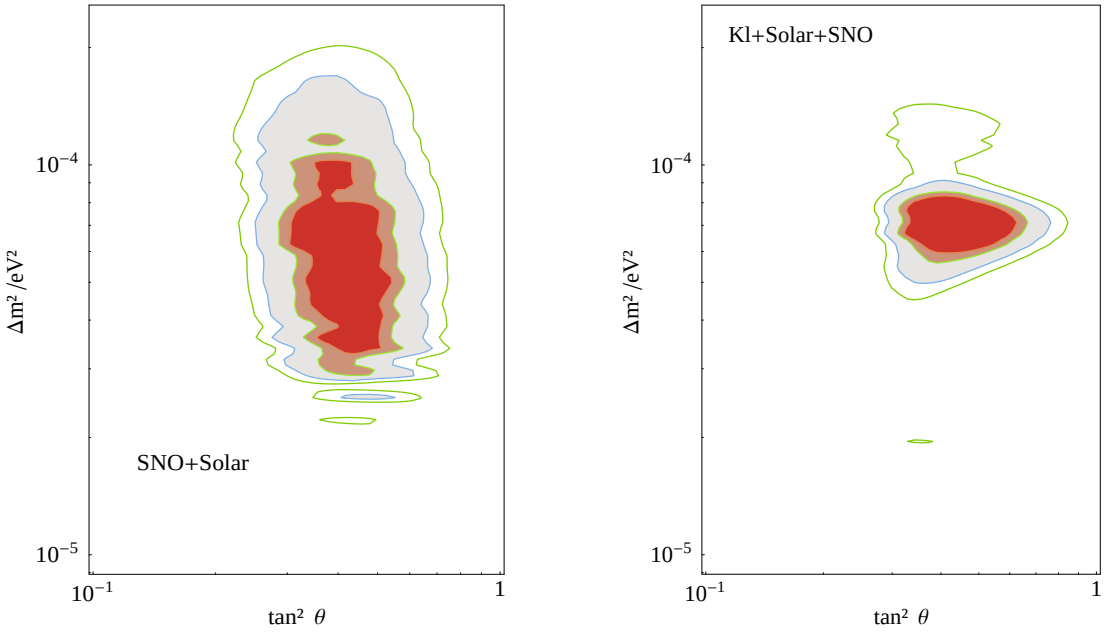


**Figure 1:** Allowed areas in the two neutrino parameter space. The colored areas are the allowed regions at 90, 95, 99 and 99.7% CL relative to the absolute minimum. (Left) Solar evidence (CL,GA,SK,SNO,SNO-salt). (Right) Kamland spectrum plus solar evidence.

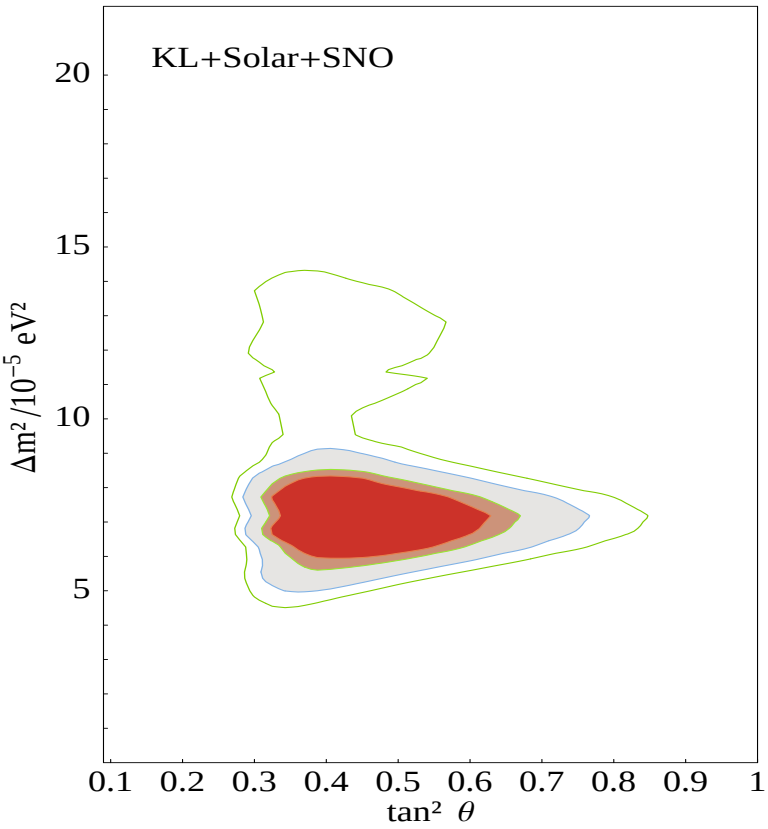


**Figure 2:** Kamland spectrum plus solar evidence as Fig.1 (right), in linear scale which allows for a better comparison between the different regions.

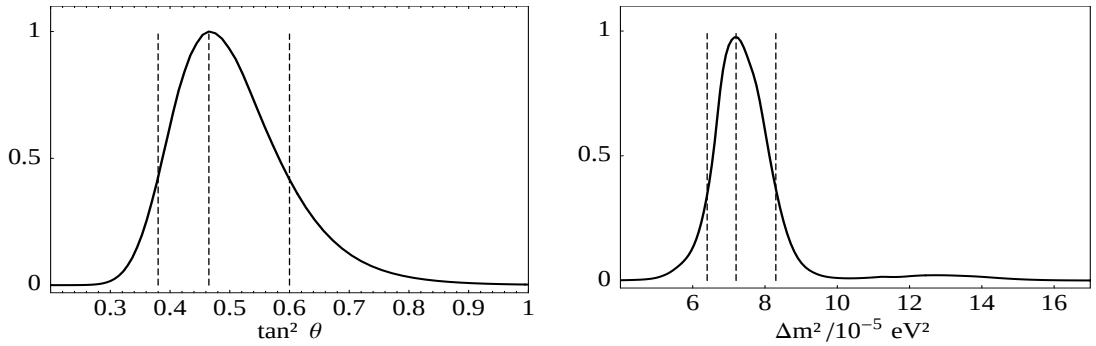


**Figure 3:** Marginalized likelihood distributions for each of the oscillation parameters $\Delta m^2$ (right), $\tan^2\theta$ (left) corresponding to the solar plus Kamland evidence (Fig.1(Right)). The curves are in arbitrary units with normalization to the maximum height. Values for the peak position are obtained by fitting two-sided Gaussian distributions (not showed in the plot). See Table 2 for values of the position and widths of the peaks.